

Stationary states of a rotating Bose-Einstein condensate: routes to vortex nucleation

K. W. Madison, F. Chevy, V. Bretin, and J. Dalibard

Laboratoire Kastler Brossel*, Département de Physique de l'École Normale Supérieure
24 rue Lhomond, 75005 Paris, France

(submitted December 31, 2000)

Using a focused laser beam we stir a ^{87}Rb Bose-Einstein condensate confined in a magnetic trap. We observe that the steady states of the condensate correspond to an elliptic cloud, stationary in the rotating frame. These steady states depend nonlinearly on the stirring parameters (amplitude and frequency), and various solutions can be reached experimentally depending on the path followed in this parameter space. These states can be dynamically unstable and we observe that such instabilities lead to vortex nucleation in the condensate.

3.75.Fi, 67.40.Db, 32.80.Lg

Superfluidity, originally discovered and studied in the context of superconductors and later in the system of superfluid liquid Helium, is a hallmark property of interacting quantum fluids and encompasses a whole class of fundamental phenomena [1,2]. With the achievement of Bose-Einstein condensation in atomic gases [3], it became possible to study these phenomena in an extremely dilute quantum fluid, thus helping to bridge the gap between theoretical studies, only tractable in dilute systems, and experiments. One striking consequence of superfluidity is the response of a quantum fluid to a rotating perturbation. In contrast to a normal fluid, which at thermal equilibrium will rotate like a solid body with the perturbation, the thermodynamically stable state of a superfluid involves no circulation, unless the frequency of the perturbation is larger than some critical frequency, analogous to the critical velocity [1]. Moreover, when the superfluid does circulate, it can only do so by forming vortices in which the condensate density vanishes and for which the velocity field flow evaluated around a closed contour is quantized.

In this Letter we present the study of the response of a Bose-Einstein condensate (BEC) confined in a magnetic trap to a rotating perturbation created by a stirring laser beam. We observe that for a given perturbation amplitude and frequency the steady state of the condensate corresponds to an elliptic cloud, stationary in the rotating frame as predicted in [4]. Depending on the path followed in the parameter space (amplitude and frequency) of the rotating perturbation, we show that two steady states can exist, corresponding to different ellipticities of the cloud. We also observe that these states possess an intrinsic dynamical instability [4,5]; moreover, we find that

this instability can lead to the transformation of the elliptic state into a state of one or more vortices. The fact that vortex nucleation seems to occur only via a dynamic instability (apart from the phase printing method explored in [6]) explains why the frequency range over which vortices are generated is notably smaller than that expected from thermodynamics ([7] and references within).

A dilute, interacting Bose gas with a large number of atoms is well described at low temperature by the hydrodynamic equations for a superfluid [8]. These equations were studied in the case of a dilute BEC in a rotating harmonic trap characterized by the trap frequencies ω_X , ω_Y , ω_z [4] (see also [9]). The axes X, Y rotate at the frequency Ω around the z axis. There exist solutions for which the BEC wavefunction is given by

$$\Psi = \sqrt{\rho} \exp\left(\frac{m}{\hbar} i\alpha XY\right). \quad (1)$$

The condensate density for these solutions is a paraboloid (Thomas-Fermi profile)

$$\rho = \frac{\mu_e}{g} \left[1 - \left(\frac{X^2}{R_X^2} + \frac{Y^2}{R_Y^2} + \frac{z^2}{R_z^2} \right) \right], \quad (2)$$

where $g = 4\pi\hbar^2 a/m$ is the collisional coupling constant set by the s -wave scattering length ($a = 5.5$ nm for ^{87}Rb in the $|F = 2, m_F = 2\rangle$ ground state), m is the atomic mass, μ_e is the chemical potential in the rotating frame (the density is understood to be vanishing for $\rho \leq 0$). The XY ellipticity of the paraboloid is related to the parameter α appearing in the phase of Eq. (1)

$$\alpha = \Omega \frac{R_X^2 - R_Y^2}{R_X^2 + R_Y^2}. \quad (3)$$

The value for α is determined by the parameters of the rotating perturbation according to

$$\tilde{\alpha}^3 + \tilde{\alpha}(1 - 2\tilde{\Omega}^2) + \epsilon\tilde{\Omega} = 0, \quad (4)$$

where $\tilde{\alpha} = \alpha/\bar{\omega}$, $\tilde{\Omega} = \Omega/\bar{\omega}$, $\bar{\omega} = \sqrt{(\omega_X^2 + \omega_Y^2)/2}$, and the trap deformation $\epsilon = (\omega_X^2 - \omega_Y^2)/(\omega_X^2 + \omega_Y^2)$. There are up to three possible values for $\tilde{\alpha}$ corresponding to stationary states of the condensate for a given pair $(\tilde{\Omega}, \epsilon)$. These solutions are plotted as lines in Figs. 1 and 2. When $\tilde{\Omega}$ varies with a fixed ϵ (Fig. 1), or when ϵ varies with a fixed $\tilde{\Omega}$ (Fig. 2), the possible values of $\tilde{\alpha}$ are located on two branches. Branch I is a monotonic function of $\tilde{\Omega}$ or ϵ , while branch II exists only for some range of the

parameters and exhibits a “back bending”, opening the possibility for hysteretic behavior.

The experimental study of these states relies on the realization of a rotating harmonic potential and a measurement of the density profile of the condensate cloud. The atoms are confined in an Ioffe-Pritchard magnetic trap which provides a static, axisymmetric harmonic potential of the form $U(\mathbf{r}) = m\omega_t^2(x^2 + y^2)/2 + m\omega_z^2z^2/2$. The condensate in this potential is cigar-shaped with a length to diameter aspect ratio of $\lambda = \omega_t/\omega_z$ which was varied between 10 and 25 ($\omega_z/2\pi = 11.8 \pm 0.1$ Hz). The atomic cloud is stirred by a focused 500 μW laser beam of wavelength 852 nm and waist $w_0 = 20\mu\text{m}$, whose position is controlled using acousto-optic deflectors [7] (see also [10]). The beam creates an optical-dipole potential which can be approximated by $m\omega_t^2(\epsilon_X X^2 + \epsilon_Y Y^2)/2$. The XY axes of the optical potential are rotated at a frequency Ω producing a rotating harmonic trap characterized by the three trap frequencies $\omega_{X,Y}^2 = \omega_t^2(1 + \epsilon_{X,Y})$ and ω_z . The value of the transverse trap frequencies is measured directly by determining the frequency domain ($\omega_Y < \Omega < \omega_X$) in which the center of mass motion of the cloud becomes dynamically unstable. This measurement provides a determination of ϵ and $\bar{\omega} = \sqrt{(\omega_X^2 + \omega_Y^2)}/2$.

To measure the state of the condensate, characterized by α , we perform a field-free expansion of the condensate for a duration of 25 ms, followed by resonant absorption imaging technique along the stirring axis [11]. Using the formalism presented in [12], we have checked that the value of α for the rotating states described by Eq. (1) changes by less than 10% during the expansion for the parameter range studied.

The experimental procedure begins with the preparation of a condensate in the pure magnetic potential by a radio-frequency (rf) forced-evaporation ramp lasting 25 s. Starting with 10^8 atoms precooled to 10 μK in an optical molasses, the atomic cloud reaches the critical temperature $T_c \sim 500$ nK with an atom number of $\sim 2.5 \cdot 10^6$. The evaporation is continued below T_c to a temperature of or below 100 nK at which point $3 (\pm 0.7) \cdot 10^5$ atoms are left in the condensate. The rf frequency is then raised to a value 20 kHz above $\nu_{\text{rf}}^{\text{min}}$, the rf frequency which corresponds to the bottom of the magnetic potential. This rf drive is kept present in order to hold the temperature approximately constant. At this point, the stirring laser is switched on and the condensate is allowed to evolve in the combined magnetic and optical potential for a controlled duration after which we perform the field free expansion and optical detection.

Since the condensate is first created in a static harmonic potential and then the rotating perturbation is introduced, the final state of the condensate depends on its evolution in a time-dependent rotating potential characterized by the two parameters $\epsilon(t)$ and $\tilde{\Omega}(t)$. If the time dependencies are slow enough, the condensate at every instant is in a stationary state corresponding to the in-

stantaneous values of ϵ and $\tilde{\Omega}$. In this case, the initial state of the condensate is $\tilde{\alpha} = 0$, and as ϵ and $\tilde{\Omega}$ evolve so does $\tilde{\alpha}$ evolve along a path defined by Eq. (4).

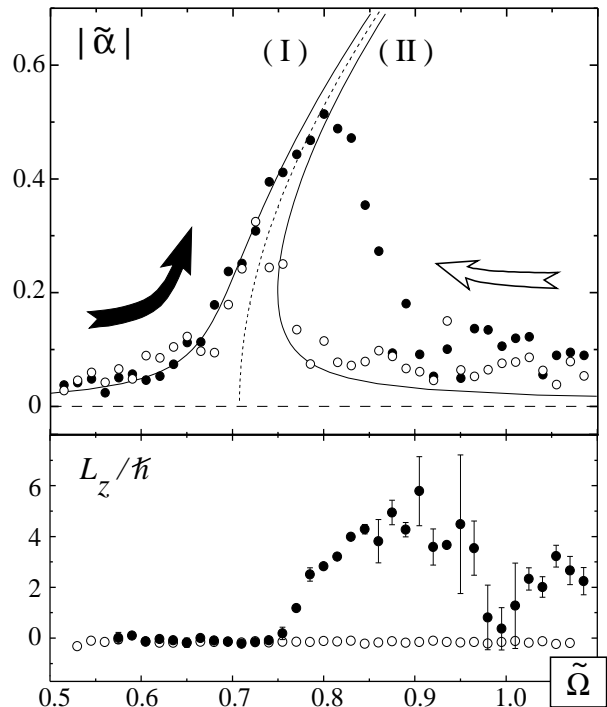


FIG. 1. Steady state value of $\tilde{\alpha}$ as a function of stirring frequency $\tilde{\Omega}$. The results of the ascending ramp are shown by a filled dot (●) and of the descending ramp by a hollow dot (○). The branches of Eq. (4) for $\epsilon = 0$ are shown as dashed lines. The best agreement between theory and experiment was achieved for all data in Figs. 1 and 2 with $\epsilon = 0.022$ and a scaling of $\bar{\omega}/2\pi = 200$ Hz, while the measured values are $\epsilon = 0.025 \pm 0.005$ and $\bar{\omega}/2\pi = 195 \pm 1$ Hz. This 2% discrepancy in the frequency may be due to a deviation from the Thomas Fermi limit. The angular momentum of the condensate measured after a 200 ms relaxation time reveals the presence of vortices for the ascending ramp above $\tilde{\Omega} = 0.75$.

The first study that we performed involved switching on the optical potential with a fixed value of $\epsilon = 0.025 \pm 0.005$ and an initial frequency of $\tilde{\Omega} = 0$. The frequency $\tilde{\Omega}$ was increased at a constant rate to a final value in the range (0.5, 1.5) [13]. The rotation frequency was then held constant at this final value during 5 rotation periods, and finally the state of the condensate was measured. For each final frequency studied, two different measurements were performed: a determination of α made according to Eq. (3) and a measurement of the angular momentum of the condensate associated with the presence of a vortex. The latter measurement, which relies on the excitation of a quadrupolar oscillation [14,15], is performed 200 ms after the stirring anisotropy is switched off. This delay is (i) short compared to the vortex lifetime [7] and (ii) long compared to the measured relaxation time (~ 25 ms) of the ellipticity of the

rotating condensate. Hence a nonzero value of L_z in this measurement is the signature of vortex nucleation. Each measurement relies on a destructive resonant-absorption imaging, and is performed independently; the results are shown in Fig. 1. We repeated the above study with a descending frequency ramp starting above 1 and finishing in the same range as the ascending ramp, and the results are also shown in Fig. 1.

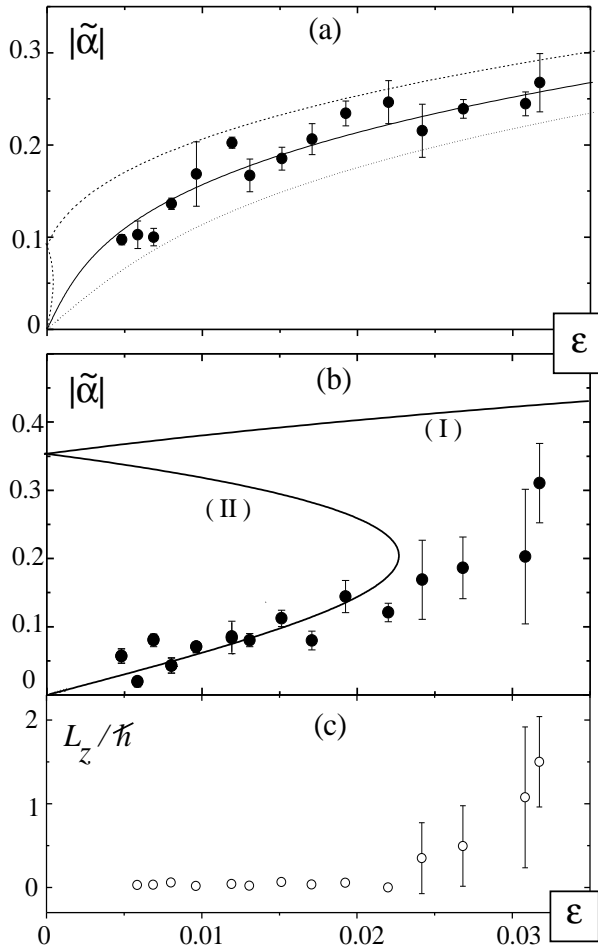


FIG. 2. Measurement of the steady state value of $\tilde{\alpha}$ obtained from a linear ramp of the stirring anisotropy for two different stirring frequencies. (a) When $\tilde{\Omega} = 0.70$ the condensate follows branch I and no vortices are nucleated. Branch I of Eq. (4) is plotted for $\tilde{\omega}/2\pi = 200$ Hz (solid line) and also for $\tilde{\omega}/2\pi = 197$ Hz and $\tilde{\omega}/2\pi = 203$ Hz (dotted and dashed lines). (b) When $\tilde{\Omega} = 0.75$ branch II is followed to the point of back bending ($\epsilon_c = 0.023$). The solid line represents the solutions of Eq. (4) for $\tilde{\omega}/2\pi = 200$ Hz. (c) For ramps which pass this point the angular momentum measured after a 200 ms relaxation time reveals that vortices are nucleated.

In both cases, the state of the condensate starts on and follows one of the branches of Eq. (4). For the descending ramp, the lower part of branch II is followed until the back bending frequency is reached below which this branch ceases to be a solution of Eq. 4. At this point, the

condensate is observed to switch to branch I and to follow it down to $\tilde{\Omega} = 0$. The fact that no vortices are nucleated along this path seems to confirm the prediction that the lower part of branch II is stable [4]. For the ascending ramp the condensate is observed to start on and to follow branch I until a frequency of $\tilde{\Omega}_c \simeq 0.75$ is reached. Beyond this point the experimentally determined value of α is no longer a solution of Eq. (4), and the presence of vortices is detected in the angular momentum measurement of the condensate. The value of $\tilde{\Omega}_c$ is in good agreement with the frequency at which branch I is expected to become dynamically unstable [5]. This experiment was repeated for different trap geometries with λ between 10 and 25 and the results were unchanged. This shows that the thermodynamic instability of the vortex state predicted to occur in a very elongated geometry ($\lambda > 15$) with $\tilde{\Omega} \sim 0.75$ does not prevent vortex nucleation [16].

In the second study that we present, the stirring frequency Ω was fixed and the rotating deformation parameter ϵ was increased linearly from zero to a final value in the range (0.005, 0.032) at a constant rate $\dot{\epsilon} = 0.078 \text{ s}^{-1}$. Then, as before, we measured either $\tilde{\alpha}$ or we checked for vortex nucleation. In this case, since α is initially zero, the branch that is followed depends on which side of the quadrupole oscillation resonance ($\tilde{\omega}/\sqrt{2}$) is Ω (see the dotted line in Fig. 1 corresponding to $\epsilon = 0$). The results are shown in Fig. 2, and we observe that when $\tilde{\Omega} = 0.7$ the condensate follows branch I. No vortices are nucleated in this case which is in agreement with the predicted stability of this branch [17]. By contrast, when $\tilde{\Omega} = 0.75$ the condensate follows the lower part of branch II up to a value of $\epsilon_c = 0.023$ where branch II bends backwards. Beyond this point the measured value of $\tilde{\alpha}$ is no longer a solution of Eq. (4) and we observe the nucleation of vortices. This situation is quite different from the one observed in the descending frequency ramp discussed above. In that case, when the back bending of branch II is reached no vortices are nucleated and the condensate is observed to switch to branch I.

In this second procedure, where $\tilde{\Omega}$ is fixed and ϵ increases slowly, the critical value ϵ_c at which the back bending of branch II occurs increases with increasing $\tilde{\Omega}$. This route can lead to vortex nucleation only if the final value of the ramp in ϵ is above ϵ_c , which for a given ramp, puts an upper limit on the stirring frequency leading to vortex formation. This is well confirmed experimentally; more precisely, with our maximal value of $\epsilon = 0.032$, we could nucleate vortices only when the stirring frequency was in the range $0.71 \leq \tilde{\Omega} \leq 0.77$.

A third route to vortex nucleation is followed when the stirring potential is switched on rapidly (~ 20 ms) and held constant for 300 ms with a fixed stirring frequency [7,14]. In particular, we found that vortices are nucleated along this route for $\tilde{\Omega} = 0.70$ and $\epsilon = 0.032$ (final parameters in Fig. 2a) in marked contrast with the results of a slow ramp of ϵ . In this case, the state of the BEC cannot

follow the sudden change in ϵ . To illustrate the nonstationary nature of the condensate we have plotted in Fig. 3 a typical time dependence of $\tilde{\alpha}$ with this nucleation procedure. We observe that $\tilde{\alpha}$ oscillates around 0.3 during the first 200 ms, and then falls dramatically to a fixed value below 0.1 at which point we see vortices entering the condensate from the border and settling into a lattice configuration. We should point out that the presence of the rotating anisotropy is not necessary beyond the first ~ 80 ms for vortex nucleation and ordering; nonetheless, the number of vortices generated is an increasing function of the stirring time after this threshold.

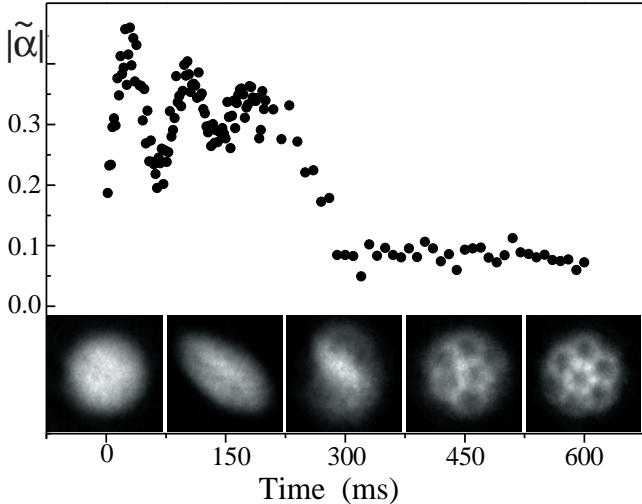


FIG. 3. Measurement of the time dependence of $\tilde{\alpha}$ when the stirring anisotropy is turned on rapidly (20 ms) to a value of $\epsilon = 0.025$ and a frequency of $\tilde{\Omega} = 0.7$ ($\lambda = 9.2$). Five images taken at intervals of 150 ms show the transverse profile of the elliptic state and reveal the nucleation and ordering of the resulting vortex lattice. The size of an image is $300\mu\text{m}$.

In conclusion, we have studied the response of a Bose-Einstein condensate confined in a magnetic trap to a rotating perturbation created by a stirring laser beam. We observe an irrotational state of the condensate which corresponds to an elliptic cloud, stationary in the rotating frame. We show that vortex nucleation in this system is related to dynamical instabilities of this irrotational state. This connection explains why the critical frequency originally observed in this system is notably larger than the one predicted by a purely thermodynamic analysis: when a vortex state is thermodynamically allowed but no dynamical instability is present, the time scale for vortex nucleation is probably too long for this process to take place in our system. A natural extension of this work is the investigation of other irrotational steady states associated with a rotating potential of a higher multipole order [10]. The exact role of temperature in vortex nucleation remains to be elucidated. We believe that it has conflicting roles in the generation of an ordered vortex lattice (see images in Fig. 3). On the one

hand, when the temperature is increased (while remaining below the condensation temperature), the ellipticity induced by the stirring is reduced and vortex nucleation is hindered and may even become impossible. On the other hand dissipation is clearly necessary to order the vortex lattice, and we observe qualitatively that the ordering time increases with decreasing temperature. We plan to address these issues in future work.

ACKNOWLEDGMENTS

We thank the ENS Laser cooling group, G. Shlyapnikov, and S. Stringari for helpful discussions. This work was partially supported by CNRS, Collège de France, DRET, DRED and EC (TMR network ERB FMRX-CT96-0002). K.M. acknowledges DEPHY for support.

* Unité de Recherche de l'École normale supérieure et de l'Université Pierre et Marie Curie, associée au CNRS.

-
- [1] E.M. Lifshitz and L. P. Pitaevskii, *Statistical Physics, Part 2*, chap. III (Butterworth-Heinemann, 1980).
 - [2] R.J. Donnelly, *Quantized Vortices in Helium II*, (Cambridge, 1991).
 - [3] For a review see e.g. *Bose-Einstein Condensation in Atomic Gases*, eds M. Inguscio, S. Stringari, and C.E. Wieman (IOS Press, Amsterdam, 1999).
 - [4] A. Recati, F. Zambelli, and S. Stringari, cond-mat/0007152.
 - [5] Y. Castin and S. Sinha, to be published.
 - [6] M.R. Matthews *et al.*, Phys. Rev. Lett. **83**, 2498 (1999).
 - [7] K. W. Madison *et al.*, Phys. Rev. Lett. **84**, 806 (2000).
 - [8] S. Stringari, Phys. Rev. Lett. **77**, 2360 (1996).
 - [9] J. García-Ripoll and V. Pérez-Carcía, cond-mat/0003451.
 - [10] R. Onofrio *et al.*, Phys. Rev. Lett. **84**, 810 (2000).
 - [11] Since the typical radial size of the condensate is only $3\mu\text{m}$, direct optical imaging is not reliable.
 - [12] P. Storey and M. Olshanii, Phys. Rev. A **62**, 33604 (2000).
 - [13] The ramp lasts for 75 periods of the final frequency and so $d\Omega/dt$ never exceeds $2\pi 550$ Hz/s. We checked that at this ramp rate the condensate follows adiabatically the branches in Fig. 1. On the other hand the frequency ramp is fast enough so that the center of mass instability does not have enough time to develop during the time that $\tilde{\Omega}$ spends in the instability region $[1 - \epsilon/2, 1 + \epsilon/2]$.
 - [14] F. Chevy, K. Madison, and J. Dalibard, Phys. Rev. Lett. **85**, 2223 (2000).
 - [15] P.C. Haljan *et al.*, cond-mat/0012320.
 - [16] D. L. Feder *et al.*, cond-mat/0009086; A. A. Svidzinsky and A.L. Fetter, cond-mat/0007139.
 - [17] Dynamical instability of this branch is expected for $\epsilon > 0.08$, well above the range explored experimentally [5].